Comprehensive two-dimensional liquid chromatography of heavy oil

van Beek, F.T.; Edam, R.; Pirok, B.W.J.; Genuit, W.J.L.; Schoenmakers, P.J.

DOI
10.1016/j.chroma.2018.06.001

Publication date
2018

Document Version
Final published version

Published in
Journal of Chromatography A

Journal of Chromatography A, 1564 (2018) 110–119

Contents lists available at ScienceDirect

Journal of Chromatography A

journal homepage: www.elsevier.com/locate/chroma

Comprehensive two-dimensional liquid chromatography of heavy oil

Fleur T. van Beek[a,b,*], Rob Edam[c], Bob W.J. Pirok[a,b], Wim J.L. Genuit[c], Peter J. Schoenmakers[a]

[a] Universiteit van Amsterdam, Van' t Hoff Institute for Molecular Sciences, Analytical-Chemistry Group, Science Park 904, 1098 XH, Amsterdam, The Netherlands
[b] TI-COAST, Science Park 904, 1098 XH Amsterdam, The Netherlands
[c] Shell Global Solutions International B.V., Grasweg 31, 1031 HW, Amsterdam, The Netherlands

ARTICLE INFO

Article history:
Received 22 February 2018
Received in revised form 1 June 2018
Accepted 3 June 2018
Available online 5 June 2018

Keywords:
Short residue
PAH
Vacuum distillation
De-asphalted heavy oil
PIOTR
SARA

ABSTRACT

Heavy oil refers to the part of crude oil that is not amenable to further distillation. Processing of these materials to useful products provides added value, but requires advanced technology as well as extensive characterization in order to optimize the yield of the most profitable products. The use of comprehensive two-dimensional liquid chromatography (LC × LC) was investigated for the characterization of de-asphalted short residue, also called maltenes. Initial studies were performed on a polycyclic aromatic hydrocarbon standard, an aromatic extract of hydrowax, and the fractions obtained after solvent fractionation of the maltenes. Cyanopropyl- and octadecyl-silica were used as first-dimension and second-dimension columns, respectively. The analysis of the maltenes and fractions thereof required a change in first-dimension stationary phase to biphenyl as well as an increase in modifier strength to improve recovery. The extensive characterization of maltenes with LC × LC within four hours was demonstrated.

The Program for the Interpretive Optimization of Two-dimensional Resolution (PIOTR) has been applied to aid the method development, but due to the absence of specific peaks in the chromatograms it was challenging to apply to the maltenes or its fractions. Nonetheless, an approach is suggested for resolution optimization in cases such as the present one, in which regions of co-elution are observed, rather than clearly separated peaks.

1. Introduction

A part of heavy oil is the short residue, also called vacuum residue or vacuum bottoms. This is the solid hydrocarbon that remains at the bottom of a vacuum distillation column after the volatile material has removed at reduced pressure (Fig. 1). Extracting higher value products out of this material requires additional processing using delayed coking technology, such as Exxon's Flexicoker [1] or Shell's Hycon [2]. To optimize the yield of the most profitable products from these processes, the material needs to be thoroughly characterized in order to optimize the conversion process [3]. The characterization of the short residue still has room for improvement, although optimization is definitely a challenge.

Since the molecular composition of short residue is so complex, the material is often separated before analysis into sub-fractions based on solubility behavior [4,5]. One of the main methods for this is a liquid chromatographic (LC) method known as SARA analysis, in which a hydrocarbon mixture is separated into four fractions: Saturates, Aromatics, Resins, and Asphaltenes [6]. The saturate fraction includes alkanes (paraffins) and cyclic alkanes (naphthenes). The aromatic fraction consists of molecules incorporating at least one aromatic ring. The resin fraction consists of compounds that contain heteroatoms, hence it is often referred to as the polar fraction or the "polars". This is evident by the fractionation process as the resins stick to the stationary phase until (back)flushing with a relatively polar solvent, such as dichloromethane (DCM). Asphaltenes are defined by their solubility range. They are soluble in toluene, but precipitate upon addition of excess *n*-heptane or *n*-pentane [7]. One has to be aware that SARA fractions are never completely excised from one another [8]. This remains inevitable when employing solvent fractionation. Understanding the composition of a specific SARA fraction can provide valuable insights, whilst retaining much of the sample dimensionality [9], and provide feedback for further processing of the short residues into profitable products.

* Corresponding author at: Science Park 904, Amsterdam, 1098 XH, The Netherlands.
E-mail address: F.T.vanBeek@uva.nl (F.T. van Beek).

https://doi.org/10.1016/j.chroma.2018.06.001

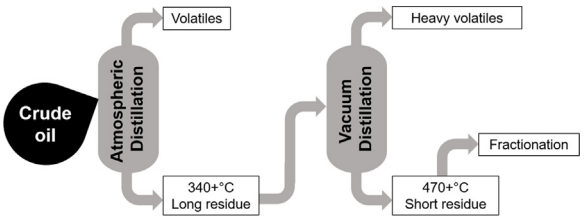

Fig. 1. Schematic of a petroleum refinery, adapted from Speight et al. [6].

For the analysis of heavy oils many techniques have been applied, including Fourier-transform ion-cyclotron-resonance mass spectrometry (FT-ICR MS) [10–12], high-temperature comprehensive two-dimensional gas chromatography (HT-GC × GC) [13,14] and comprehensive two-dimensional supercritical-fluid chromatography (SFC × SFC) [15,16]. Dutriez et al. [17] analyzed resin fractions using both FT-ICR MS and HT-GC × GC in order to compare the analytical capabilities of these techniques for heavy oils. However, as the components become heavier and less volatile, their analysis becomes more difficult. Volatility of a sample is an inherent requirement for gas chromatography (GC) and since this property decreases as the molar masses and polarity of oil components increases, GC × GC becomes more complicated and eventually impossible for materials such as short residue. FT-ICR MS is able to deal better with heavier samples, but struggles with accurate quantification and with the separation of isomeric components. Techniques like supercritical-fluid chromatography (SFC) and LC are better suited for characterizing short residue, since they do not require volatile analytes. Nevertheless, the analysis of heavy components heavier than C_{90} is troublesome for SFC [16].

While one-dimensional liquid chromatography (1D-LC) is most often employed for sample preparation and fractionation of heavy hydrocarbons, comprehensive component analysis is impossible due to broad, unresolved peaks in the chromatogram caused by the molecular complexity of the sample [18,19]. The purpose of this work is to determine if comprehensive two-dimensional liquid chromatography (LC × LC) could be a possible alternative approach.

LC × LC is a method in which the first-dimension (^{1}D) chromatographic column is coupled to a second-dimension (^{2}D) chromatographic column through a switching valve or another transferring device in order to subject the entire ^{1}D effluent to ^{2}D separations [20,21]. The effluent from the ^{1}D should be sampled 2–4 times over the 4-σ width of the ^{1}D peak to ensure two-dimensional resolution [22,23]. In LC × LC the peak capacities of the two dimensions can ideally be multiplied, giving rise to an immense increase in separation power [18,23,24]. In order to deal with complex samples that require more peak capacity than an LC method can offer, LC × LC seems to provide good prospects. Duarte et al. [25] applied LC × LC on natural organic matter, where 1D-LC could not handle the sample complexity, and showed great improvement in their ability to resolve individual components in the sample. Similarly, Murahashi [26] performed LC × LC on polycyclic aromatic hydrocarbons (PAHs) in environmental samples and showed that the technique provided valuable additional information. More specifically, Jakobsen et al. [27] applied LC × LC with pulsed elution of the first dimension to a heavy oil fraction of vacuum gas oil and coker gas oil.

Nevertheless, the advantages of the additional dimension in LC × LC come at the cost of significantly more complicated method development [21,28–30]. As the two columns are coupled through a modulation device, often consisting of a switching valve and two loops that are filled and emptied consecutively, the optimization of both separations is no longer independent. Similar to 1D-LC, LC × LC also requires optimization of individual parameters, such as column dimensions, particle size, flow rate, mobile-phase composition, temperature, pH, *etc.* In addition, LC × LC requires the compatibility of the two dimensions and the way they are connected to be considered, *i.e.* modulation time and the effects of the ^{1}D effluent on the ^{2}D separation [31]. Recently described software called "Program for Interpretive Optimization of Two-dimensional Resolution" (PIOTR) developed by Pirok et al. [32] was shown to speed up LC × LC method development, based on only a few experiments, taking into account the retention behavior of the analytes under varying isocratic or gradient mobile-phase conditions.

Vanhoenacker et al. [33] achieved a separation of a petroleum short residue by multiple-heart-cut two-dimensional liquid chromatography (2D-LC), using a combination of normal-phase LC (NPLC) and reversed-phase LC (RPLC). Although they were specifically interested in the quantification of PAHs to deal with regulations, their work suggested that comprehensive two-dimensional separation of short residues could provide a more complete overview of sample composition. In fact, Vanhoenacker et al. [34] investigated LC × LC of the aromatic fraction of mineral oil after liquid-liquid extraction using *n*-hexane and nitromethane. Although this method provided more comprehensive information on the sample, the mineral-oil fraction studied was probably still light enough to enable analysis by the previously mentioned methods, *i.e.* FT-ICR/MS and HT-GC × GC, which are more mature and already used routinely. To the authors' knowledge the application of LC × LC to short residue fractions has not been reported previously.

In this work, an LC × LC method has been developed to separate the saturate, aromatic and resin fractions of de-asphalted short residue in order to provide feedback for oil processing. To streamline method development and to test the efficacy of the available software, PIOTR [32] was applied in the current work.

2. Material and methods

2.1. Instrumental

The main instrument used in this study was an Agilent 1290 Infinity II 2D-LC Solution (Agilent, Germany). The system included two binary pumps (G7120 A) with V35 Jet Weaver mixers (G4220-60006), a multisampler (G71678), two thermostatted column compartments (G71168) equipped with a 2-pos/6-port valve (5067-4137) and 2-pos/8-port valve (5067-4214) fitted with two 40-μL loops, and a diode-array detector (DAD; G7117B) fitted with a Max-Light Cell (G4212-60008). After the DAD a Thermo Scientific Dionex Corona Veo RS charged-aerosol detector (CAD) was attached, through a T-piece with a pressure release (G4212-68001), which communicated with the system through a transformer box (G13908).

An Agilent stable-bond cyanopropyl column (CN; 100 × 2.1 mm, 3.5 μm), or a Phenomenex Kinetex pentafluorophenyl column (F5; 100 × 3.0 mm, 2.6 μm), or a Phenomenex Kinetex biphenyl column (BiPh; 100 × 3.0 mm, 2.6 μm) was used in the first dimension. An Agilent Zorbax RRHD Eclipse PAH column (C_{18}; 50 × 3.0 mm, 1.8 μm) was used in the second dimension.

The system was controlled by Agilent OpenLAB CDS Chemstation Edition A02.02 software. Data were collected using Agilent OpenLAB CDS ChemStation Edition for LC & LC/MS Systems, Version C.01.07 [27] with Agilent 1290 Infinity 2D-LC Software, Version A.01.02[025]. Data was processed using MatLAB R2015a version 8.5.0.197613 (Mathworks, Woodshole, MA, USA).

2.2. Chemicals

2-Propanol (IPA, gradient grade), acetonitrile (ACN, Reag. Ph Eur gradient grade), dichloromethane (DCM, for liquid chromatogra-

phy), methanol (MeOH, Reag. Ph Eur gradient grade), and toluene (for liquid chromatography) were LiChrosolv purchased from Merck (Darmstadt, Germany). Deionized water was prepared using a MilliQ Integral A-10 system from Merck.

2.3. Samples

The oil samples were obtained from Shell Global Solutions International B.V. in Amsterdam, The Netherlands. After asphaltene removal according to ASTM method D3279 [7], the remaining deasphalted short residue, referred to as maltenes, was fractionated according to an in-house SARA fractionation method to obtain the saturate, aromatic and resin fractions. The samples were dissolved in toluene to a concentration of 20 mg/mL. The aromatic extract of hydrowax (HW) was obtained by liquid-liquid extraction with DMSO. A 24-component polycyclic aromatic hydrocarbon standard mix, as tested in EPA method 610 (PAH610), was obtained from Accustandard (p.n. M-8100-QC, New Haven, Connecticut, USA). This PAH610 standard contained polycyclic aromatic hydrocarbons ranging from 2-ringed structures up to 6-ringed structures, including a few nitrated and methylated compounds.

2.4. Methods

2.4.1. 1D-LC methods

For comparison of the ^{1}D stationary phases the column ovens were set to 40 °C and the acquisition rate of the DAD was set to 80 Hz, with a 4 nm slit width to collect data at wavelengths of 220, 254, 280, 305, 340, and 500 nm. The injection volume was 0.1 μL. Different mobile-phase compositions were used; water (A) and ACN (B), water (A) and MeOH (B), or water/MeOH 50:50 (v/v) (A) and THF (B) for the respective investigations into modifier influence.

The BiPh and F5 columns were used at a flow rate of 0.6 mL/min. For the modifiers ACN and MeOH the gradient programs were: 0–0.05 min, isocratic at 50%B; 0.05–32.05 min, linear gradient to 100%B; 32.05–55 min, isocratic at 100%B; 55–56 min, linear gradient to 50%B; 56–60 min, isocratic at 50%B. For the THF modifier, the gradient program was somewhat different to reflect the greater eluent strength of solvent A: 0–0.05 min, isocratic at 100%A; 0.05–32.05 min, linear gradient to 100%B; 32.05–55 min, isocratic at 100%B; 55–56 min, linear gradient to 100%A; 56–60 min, isocratic at 100%A.

Due to a lower maximum pressure tolerance of the CN column compared to the BiPh and F5 columns a flow rate of 0.4 mL/min was used when testing the CN column. In order to keep the number of column volumes consistent with those of the other columns, the gradient programs for the modifiers ACN and MeOH were: 0–0.04 min, isocratic at 50%B; 0.04–23.6 min, linear gradient to 100%B; 23.6–40.4 min, isocratic at 100%B; 40.4–41.1 min, linear gradient to 50%B; 41.1–44.1 min, isocratic at 50%B. Again accounting for the greater eluent strength, the gradient program for the THF modifier was: 0–0.04 min, isocratic at 100%A; 0.04–23.6 min, linear gradient to 100%B; 23.6–40.4 min, isocratic at 100%B; 40.4–41.1 min, linear gradient to 100%A; 41.1–44.1 min, isocratic at 100%A.

The 1D-LC separation of HW was performed at 40 °C with a flow rate of 0.85 mL/min on the C_{18} column (see Section 2.1). The acquisition rate of the DAD was set to 80 Hz with a 4 nm slit width to collect at wavelengths of 220 nm and 340 nm. The injection volume was 0.1 μL. The mobile phase consisted of water (A) and ACN (B), which were combined in a gradient program: 0-0.05 min, isocratic at 40%B; 0.05–12 min, linear gradient to 100%B; 12–18 min, isocratic at 100%B; 18–20 min, linear gradient to 40%B; 20–24 min, isocratic at 40%B.

2.4.2. LC × LC of aromatic extract of hydrowax and aromatic fraction of maltenes

The initial LC × LC method, applied to the HW sample and the aromatic fraction of maltenes, employed a CN and a C_{18} stationary phase in the ^{1}D and ^{2}D, respectively. The dwell volumes for the ^{1}D and ^{2}D were 174 μL and 190 μL respectively. UV data were recorded at 220, 254, 280, 305, 340 nm at 80 Hz and CAD data was recorded at 100 Hz in the 0–500 pA range. The injection volume was set to 1.0 μL. The temperature of both thermostatted column compartments was set to 40 °C. The ^{1}D mobile phase was water (A) and ACN (B). The flow rate was set to 20 μL/min with the following a gradient program: 0–2 min, isocratic at 50%B; 2–242 min, linear gradient to 100%B; 242–332 min, isocratic at 100%B; 332–338 min, linear gradient to 50%B; 338–355 min, isocratic at 50%B. The ^{2}D mobile phase was MeOH (A) and DCM (B). The flow rate was set to 2.0 mL/min with the following gradient program: 0–1.3 min, linear gradient from 0% to 65%B; 1.3–1.35 min, linear gradient to 100%A; 1.35–1.5 min, isocratic at 100%A. This gradient was repeated from 0 to 337.5 min of the analysis with a modulation time of 1.5 min.

2.4.3. LC × LC for PIOTR

For both the HW and PAH610, the same methods were used to generate peak data as input for PIOTR. Both methods were performed at 40 °C employing a CN and a C_{18} stationary phase as ^{1}D and ^{2}D, respectively. The injection volume of HW and PAH610 were 1.0 μL and 0.5 μL respectively. UV data was recorded at 220, 254, 280, 305, 340, and 500 nm at 80 Hz and CAD data was recorded at 25 Hz in a 0–500 pA range. The ^{1}D used water (A) and ACN (B) at a flow rate of 10 μL/min, whilst the ^{2}D used MeOH (A) and DCM/MeOH 90:10 (v/v) (B) at a flow rate of 2.0 mL/min.

For the 'fast' PIOTR method employing a steep gradient, the ^{1}D gradient was programmed to 180 min: 0–2 min, isocratic at 50%B; 2–150 min, linear gradient to 100%B; 150–167 min, isocratic at 100%B; 167–175 min, linear gradient to 50%B; 175–180 min, isocratic at 50%B. The ^{2}D was programmed to modulate up to 180 min with a modulation time of 1 min: 0-0.9 min, linear gradient from 100%A to 100%B; 0.9-0.95 min, linear gradient to 100%A; 0.95–1 min, isocratic at 100%A.

For the 'slow' PIOTR method employing a shallower gradient, the ^{1}D gradient was programmed to 540 min: 0–2 min, isocratic at 50%B; 2–450 min, linear gradient to 100%B; 450–500 min, isocratic at 100%B; 500–525 min, linear gradient to 50%B; 525–540 min, isocratic at 50%B. The ^{2}D was programmed to modulate up to 540 min with a modulation time of 3 min: 0–2.7 min, linear gradient from 100%A to 100%B; 2.7–2.85 min, linear gradient to 100%A; 2.85–3 min, isocratic at 100%A.

2.4.4. Optimum LC × LC method for aromatic extract of hydrowax

The optimum method determined by PIOTR, applied to HW was performed using the same columns, mobile phases, injection volume, and data acquisition conditions as those applied in the PIOTR experiments (see Section 2.4.3). The ^{1}D flow rate was set to 15 μL/min with the following a gradient program: 0–1 min, isocratic at 50%B; 1–101 min, linear gradient to 100%B; 101–158 min, isocratic at 100%B; 158–159 min, linear gradient to 50%B; 159–160 min, isocratic at 50%B. The ^{2}D flow rate remained the same at 2.0 mL/min but now followed the gradient program: 0-0.2 min, isocratic at 100%A; 0.2–1.2 min, linear gradient to 11%B; 1.2–1.4 min, linear gradient to 100%B; 1.4–1.92 min, isocratic at 100%B; 1.92–1.95 min, linear gradient to 100%A; 1.95–2 min, isocratic at 100%A. This gradient was repeated from 0 to 160 min of the analysis with a modulation time of 2 min.

2.4.5. Optimum LC × LC method for polycyclic aromatic hydrocarbon standard PAH610

The optimum method determined by PIOTR, applied to PAH610 was also performed using the same columns, mobile phases, and data acquisition conditions as those applied in the PIOTR experiments (see Section 2.4.3). The injection volume was 1.0 μL. The ^{1}D flow rate was set to 20 μL/min with the following a gradient program: 0–10 min, isocratic at 50%B; 10–70 min, linear gradient to 70%B; 70–118 min, isocratic at 70%B; 118–119 min, linear gradient to 50%B; 119–120 min, isocratic at 50%B. The ^{2}D flow rate again remained the same at 2.0 mL/min, but flowed the gradient program: 0-0.1 min, isocratic at 100%A; 0.1-0.95 min, linear gradient to 2.3%B; 0.95–1 min, linear gradient to 100%A. This gradient was repeated from 0 to 120 min of the analysis with a modulation time of 1 min.

2.4.6. LC × LC method for maltenes and its SARA fractions

The final LC × LC method, applied to the maltenes and its SARA fractions employed a BiPh and C_{18} stationary phase as ^{1}D and ^{2}D, respectively. The flow rates, column temperature, and data acquisition conditions were the same as those used initially (see Section 2.4.2), but the injection volume was increased to 10 μL. The ^{1}D mobile phase was MeOH (B) and THF (A) and followed the gradient program: 0–260 min, linear gradient from 0% to 100%A; 260–270 min, isocratic at 100%A; 270–275 min, linear gradient to 100%B; 275–280 min isocratic at 100%B. The ^{2}D mobile phase remained the same using of MeOH (A) and DCM/MeOH 90:10 (v/v) (B). The gradient was programmed to modulate up to 276 min with a modulation time of 1.5 min: 0–1.3 min, linear gradient from 0% to 100%B; 1.3–1.35 min, isocratic at 100%B; 1.35–1.5 min linear gradient to 0%B.

3. Results and discussion

In industry, structure-property relationships based on compositional information, beyond straightforward solvent fractionation, are crucial to successfully process short residue into useful products. In the case of short residue it is difficult to obtain meaningful information from a 1D-LC experiment. A typical 1D-LC method for heavy aromatics has been described by Fetzer et al. [35], where the large PAHs were monitored at 305 and 340 nm. Since key components to be measured co-elute with other components in 1D-LC, jeopardizing the accuracy of the analysis, LC × LC analysis was attempted in this work to improve the separation. Although the 1D-LC separation in Fig. 2A is clearly superior to the reconstituted 1D-LC of the same column in LC × LC (shown to the left of the LC × LC chromatogram in Fig. 2B), one must take into account the compromises that need to be made in order to make the LC × LC separation possible and competitive to 1D-LC. Theoretical calculation of the peak capacity in 1D-LC gives an approximate value of 50, whereas the peak capacity in LC × LC is the product of both dimensions giving an approximate peak capacity of 875. Even though the separation space is not entirely utilized, the possible gain in separation is still major. As seen in Fig. 2A, 1D-LC of HW shows a great deal of overlap between peaks and poor or no baseline resolution. The heavier components of interest, eluting after 10 min, overlap with other components and show poor baseline resolution, which makes quantification difficult. These components are clearly separated using LC × LC as seen in Fig. 2B, where the heavier components elute as peaks fully resolved from the bulk. Therefore, a two-dimensional approach may result in more-accurate identification and quantitation of the high-molecular-mass aromatics.

3.1. Optimization of separations of PAH610 and HW using PIOTR

Although applying an LC × LC method to HW showed that this can provide added value, optimizing such a method takes a long time. This is not favourable in industry. A sub-optimal, robust and reliable method may often be accepted, avoiding the costs associated with optimizing a method during several months. This is one of the reasons for which the “Program for Interpretive Optimization of Two-dimensional Resolution” (PIOTR) was developed by Pirok et al. [32]. The program requires retention data of a number of compounds of interest obtained from two LC × LC chromatograms with sufficiently different gradient slopes in each dimension to establish retention-model parameters. These parameters can be used to predict the retention times under any type of mobile-phase-composition program. The various method parameters are optimized by simulating a large number of methods, after which the analyst may assess the separation performance by evaluation of quality descriptors (*e.g.* orthogonality, resolution and analysis time) through Pareto-optimality (PO) plots. PO plots can be used to display only the Pareto front, *i.e.* those points for which the different criteria cannot all be improved simultaneously. For example, in a PO plot with analysis time and resolution as criteria, only those points are retained at which better resolution in a shorter time cannot be achieved.

It was decided to test the program on a standard PAH sample (PAH610), as well as on the HW sample. Fig. 3 shows the fast and slow chromatograms obtained for the optimization by PIOTR and the chromatogram collected after applying the optimized method to PAH610 (3 A, 3B and 3C respectively) and HW (3D, 3E, and 3 F respectively). Both of the optimized methods require a shorter analysis time. The optimized method for PAH610 clearly shows increased resolution and orthogonality, whereas the optimized method for HW mainly led to improvements in terms of analysis time and orthogonality.

Using the data from Figs. 3A, B, D and E, PO-plots were automatically generated by PIOTR for all possible combinations of input parameters, as can be seen in Fig. 4A, in which the possible outcomes for the optimization of PAH610 are depicted. The pareto-optimal front is highlighted by a red dashed line and the selected optimum method was a point on the Pareto-optimal front indicated by a yellow circle and pointed out by the arrow. This method was only one out of a range of possible methods and was selected based on a combination of resolution, orthogonality and analysis time. The optimization approach focused on the parameters of orthogonality, resolution and analysis time. The measure of resolution was calculated as described by Pirok et al. [32], in short the resolution of a peak is calculated in relation to all other peaks in the chromatogram. Since PIOTR allows the user to inspect every PO point and make a decision based on the scores and attractiveness of the chromatogram, a balance could be found between analysis time, resolution and orthogonality. The decision of selecting a point in the PO-plot remains that of the analyst and could be revisited if the validation fails or if the analytical question changes.

The experimentally obtained “optimal” method was compared with the theoretical prediction using the experiment-verification tool, which allows one to determine whether the predicted and experimental results concur or deviate significantly. Deviations between the predicted and experimental results may indicate misassignments during peak tracking, imperfect retention models or experimental variability. Fig. 4B shows the validation plot of PAH610 given by PIOTR in which the experimentally obtained peaks have been selected as points. The black circles connected to the experimental points depict the retention times of the corresponding peaks as predicted by PIOTR. The plot is supported by a validation table, seen in the supplementary information S3, which indicates the difference between the experimental and predicted

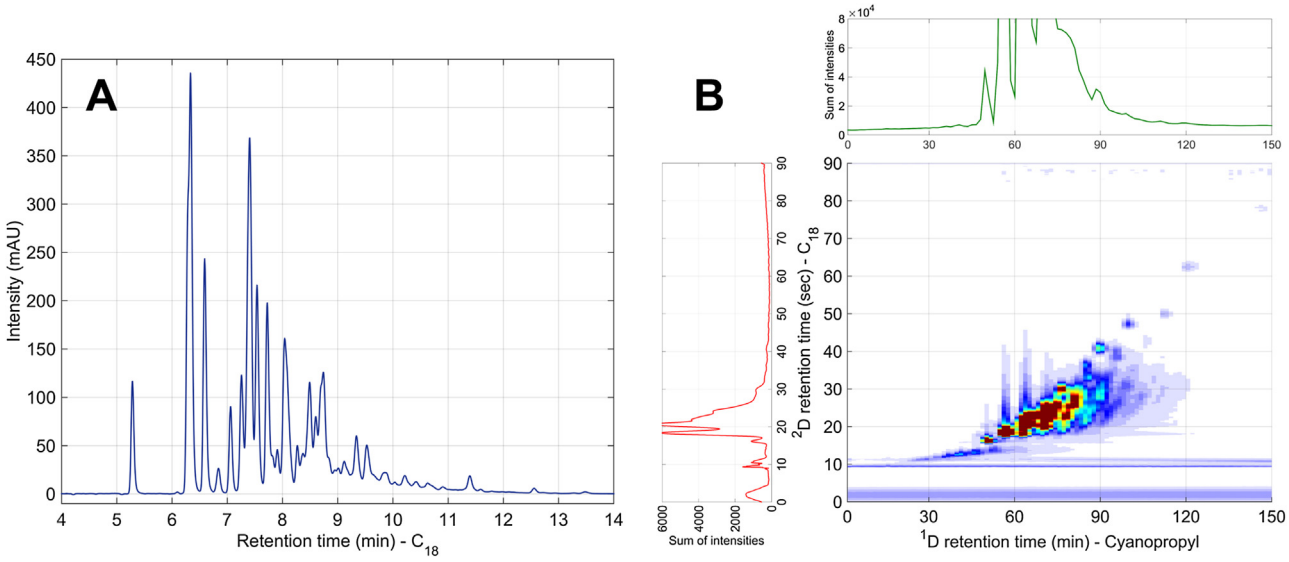

Fig. 2. (A) LC-UV chromatogram of HW shown at a detection wavelength of 340 nm, recorded according to the method described in Section 2.4.1 using the same C_{18} column as in the second dimension of the LC × LC analysis. (B) LC × LC-UV chromatogram of HW, shown at a detection wavelength of 340 nm, recorded according to the method described in Section 2.4.2. The LC-UV chromatograms to the left and top of the LC × LC chromatogram have been reconstructed from the LC × LC data. Reconstruction was performed by summing all intensities of the ^{1}D to obtain the (red) chromatogram to the left and summing all intensities of the ^{2}D to obtain the (green) chromatogram to the top. For the full chromatograms see supplementary information S1.

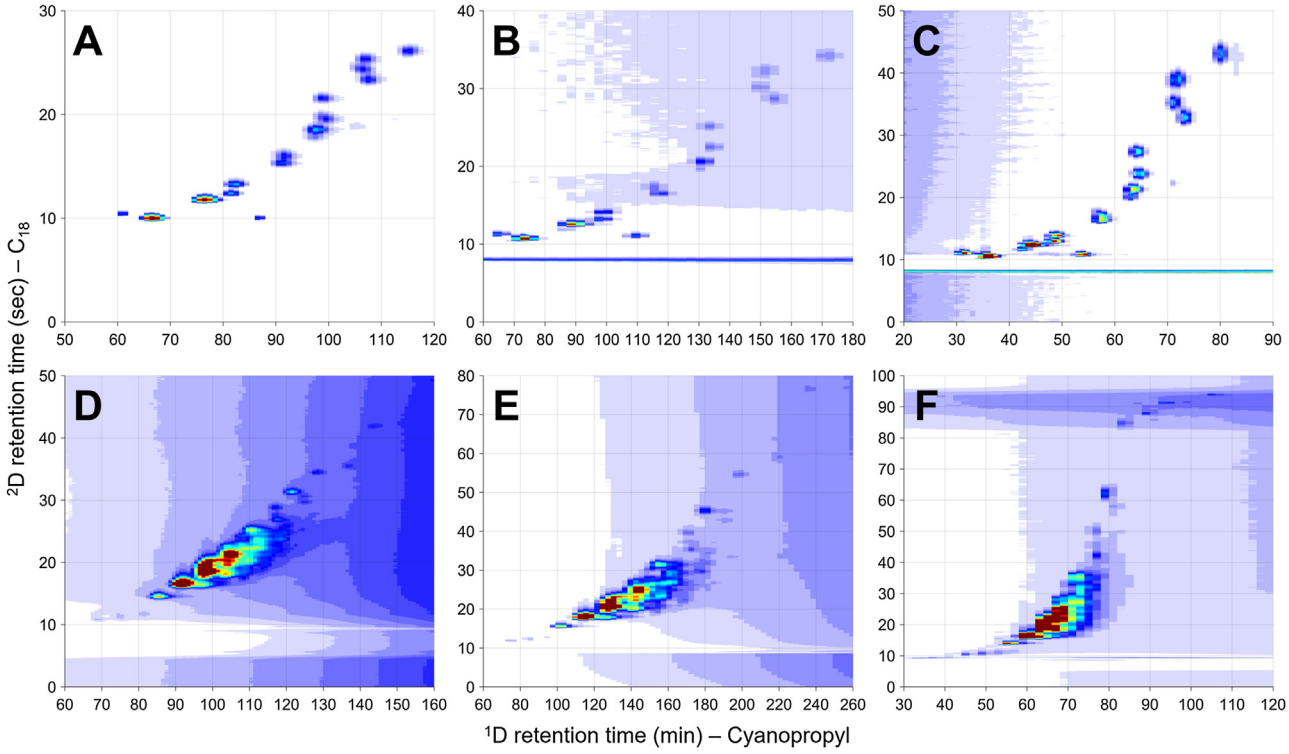

Fig. 3. LC × LC-UV chromatograms of the fast (A), slow (B), and optimized (C) separations of PAH610 and the fast (D), slow (E), and optimized (F) separations of HW, shown at a detection wavelength of 340 nm. The chromatograms were recorded according to the methods described in Sections 2.4.3, 2.4.4, and 2.4.5. For the full chromatograms see supplementary information S2.

data numerically. The differences in the current example seem to be small, except around 50 min in ^{1}D, where the experimental peaks and predicted points (depicted as black circles) are quite far apart as indicated by the long (red) lines. This may be due to the fact that the gradient parameters of the predicted optimal method were not within the domain of the scanning gradients used to determine the retention parameters, which has very recently been shown to affect the accuracy of prediction [36].

3.2. LC × LC of SARA fractions

LC × LC provides added value to the separation of HW, since many components co-eluting in 1D-LC can now be separated. When LC × LC is applied to heavier, more complex samples, such as SARA fractions the outcome may be less clear. The boiling-point range of a short residue starts at 470 °C under vacuum conditions. In this domain the numbers of isomers present ranges in the billions

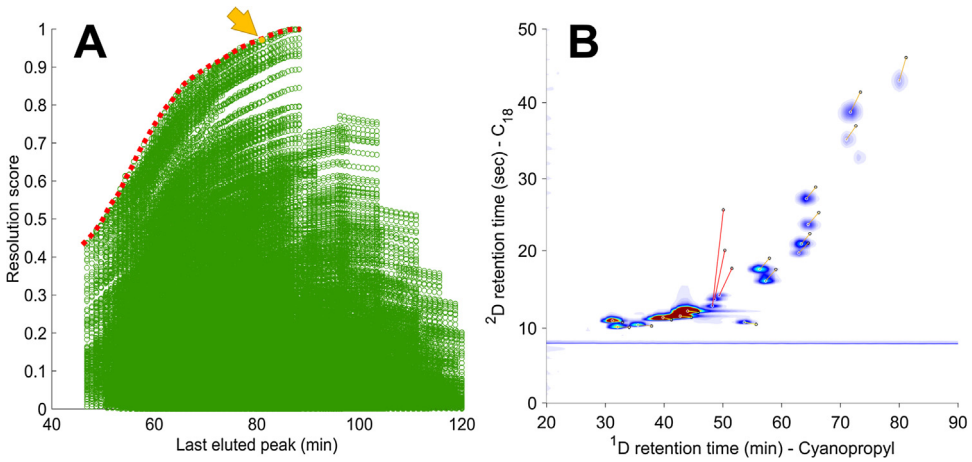

Fig. 4. (A) Pareto optimality plot for PAH610 showing the pareto-optimal front (red dashed line) and the point selected as the optimum method (yellow circle indicated with arrow). (B) LC × LC-UV chromatogram of the optimized separation of PAH610 shown at a detection wavelength of 340 nm. The black dots indicate the points at which the corresponding peaks eluted according to the prediction by PIOTR. See supplementary information S3 for the complete table of data points.

[37]. By taking the aromatic SARA fraction of a de-asphalted short residue as an intermediate sample, the number of components is reduced. However, the sample complexity remains high. Beside the many aromatic components, some saturate and resin components may still be present due to the nature of the solvent-fractionation process.

As can be seen from Fig. 5, a method similar to that applied to HW does not result in the elution of the entire aromatic SARA fraction. Nevertheless, some potentially useful separation is observed, which may reveal underlying information about the composition of this particular fraction. One can observe at least three main regions that have been separated; a fanned out pattern similar to HW indicated by the red dotted line; a broad stretched out diagonal smear; and a thin tail indicated by the pink dashed line. Further study of the fractions eluting in the different regions using MS may provide more insight in the separation, but this was not the aim of the present study. Although the identification of components in this separation was not performed, the comparison of samples from different origins may give a quick indication of the variations between them.

3.3. Stationary- and mobile-phase optimization for LC × LC of maltenes

Our aim was to analyse a maltenes sample in one run using LC × LC. Such a de-asphalted short residue contains a myriad of compounds, including apolar and polar components. These are expected to elute both before and after the components eluting from the aromatic fraction of maltenes seen in Fig. 5. To develop a method tailored to the maltenes sample, an initial optimization of stationary and mobile phases was performed. The optimization focussed on the first dimension, which was deemed to be the limiting factor with respect to the recovery of the sample. We aimed to maximize the orthogonality of the two separations, without turning to NPLC, as this would not be compatible with the RPLC second dimension. A few alternative stationary phases were compared using different modifiers. Fig. 6 shows the separation of PAH610 on a CN (red, dashed line), an F5 (green, dotted line), and a BiPh (blue, solid line) stationary phase using identical mobile-phase conditions.

To enhance the recovery, purging with a strong solvent is required. In the present case THF was investigated for this purpose. The F5 and BiPh stationary phases showed sufficient retention. The latter stationary phase was selected, since it possessed the highest column efficiency. For the performance-test results see supplementary information S4. Fig. 7 shows a comparison of the chromatograms obtained with gradients from water/MeOH 50:50 (v/v) to MeOH (red, dashed line), water/ACN 50:50 (v/v) to ACN (blue, dotted line) and MeOH to THF (green, solid line) to elute the aromatic fraction of maltenes. Although the elution window is narrowed using THF, a much greater fraction of the sample is seen to elute. The signal returns to the baseline early, suggesting complete elution of the sample. The disturbance in the signal between 1 and 5 min is due to the oversaturation of the detector from the sample solvent toluene, which is evident after subtraction of the blank. The modifier comparison is similar for the CN and F5 stationary phases, which can be seen in supplementary information S5.

Although the optimization of the first dimension was crucial to allow all of the sample to elute, the second-dimension performance was found to be adequate for application. A polymeric C_{18} stationary phase was used because of its additional shape selectivity and better resolution in comparison with typical C_{18} stationary phases, as explained by Sander and Wise [38,39].

3.4. LC × LC of maltenes

The new LC × LC method for separating the SARA fractions appeared to elute all of the components and the results, seen in Fig. 8, suggested that the fractions could be separated from each other. In order to detect the saturated components a charged-aerosol detector (CAD) was added after the UV detector. This led to the interesting observation of a bimodal distribution for the saturate fraction, which suggests significant differences between the various saturated components. Although the separation of the fractions may not seem all that great, one must realize that the number of components present is extremely high [37]. The required peak capacity to resolve all these compounds is currently impossible to reach, leading to smeared out regions rather than sharp peaks. Interestingly, the slope of the aromatics band (Figs. 8B and E) seems somewhat steeper than that of the other fractions, suggesting a higher retention of aromatic compounds on the C_{18} stationary phase.

To indicate whether it would be possible to separate the fractions of maltenes within one run, the separations were overlaid using the contours of the fractions in the CAD data, see Fig. 9A. Additionally, the maltenes sample from which the fractions were separated was injected in the LC × LC system and detected using UV, see Fig. 9B, and CAD, see Fig. 9C. From these results is can be seen that there is good separation of the saturate fraction, but that the aromatic and resin fraction still appear to co-elute. This may be

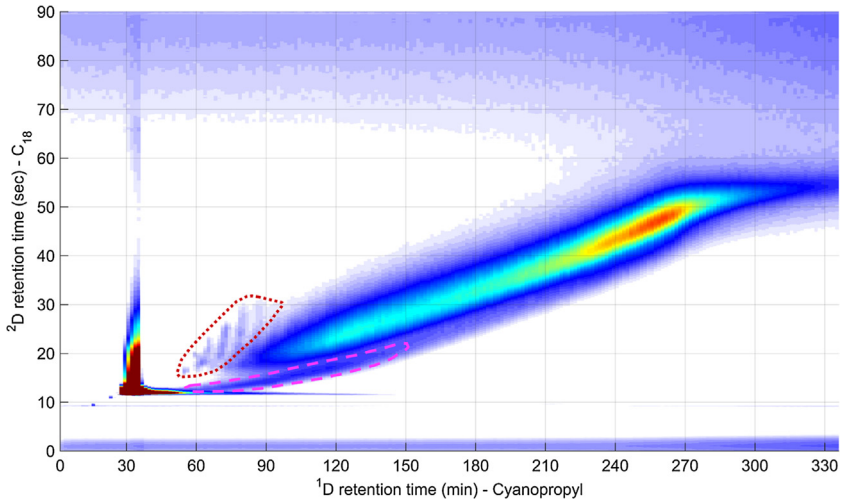

Fig. 5. LC × LC-UV chromatogram of an aromatic fraction of maltenes, recorded at a detection wavelength of 254 nm. Besides the main smear two different regions have been indicated by the red dotted line and the pink dashed line. The chromatogram was recorded according to the method described in Section 2.4.2.

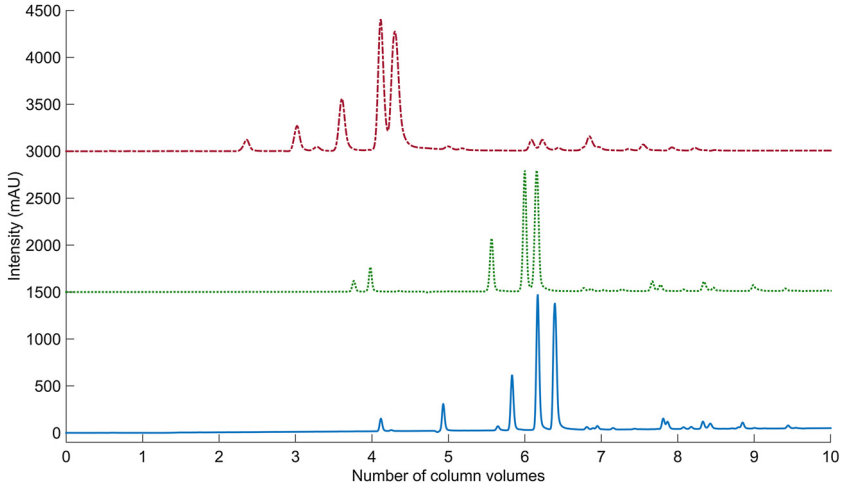

Fig. 6. LC-UV chromatograms of PAH610 separated on a CN (red, dashed line), an F5 (green, dotted line) and a BiPh (blue, solid line) stationary phase, shown at a detection wavelength of 254 nm. The separations were performed according to the methods described in Section 2.4.1. The retention axes were normalized by conversion to number of column volumes. The signal intensity of the F5 (green, dotted line) and CN (red, dashed line) measurements were increased by 1500 and 3000 mAU respectively for plotting.

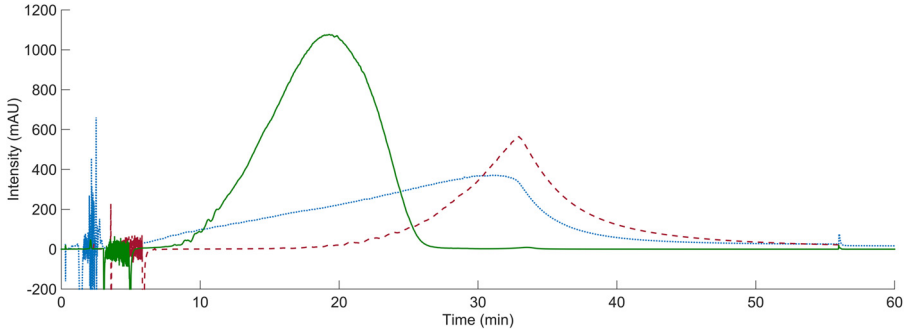

Fig. 7. LC-UV chromatograms of an aromatic fraction of maltenes, shown at a detection wavelength of 254 nm, using 60 min linear gradients from water/MeOH 50:50 (v/v) to MeOH (red, dashed line), water/ACN 50:50 (v/v) to ACN (blue, dotted line) and MeOH to THF (green, solid line). The separations were performed according to the methods described in Section 2.4.1.

explained by the sheer number of compounds present. Nevertheless, the separation power of this system, using the current column combination and conditions, seems insufficient to fully differentiate between the aromatic and resin fractions.

Optimizing the gradients of this LC × LC method could improve the separation and may slightly pull apart the different groups. However, PIOTR has never been applied to this type of sample, since it requires individual peaks to be tracked to determine

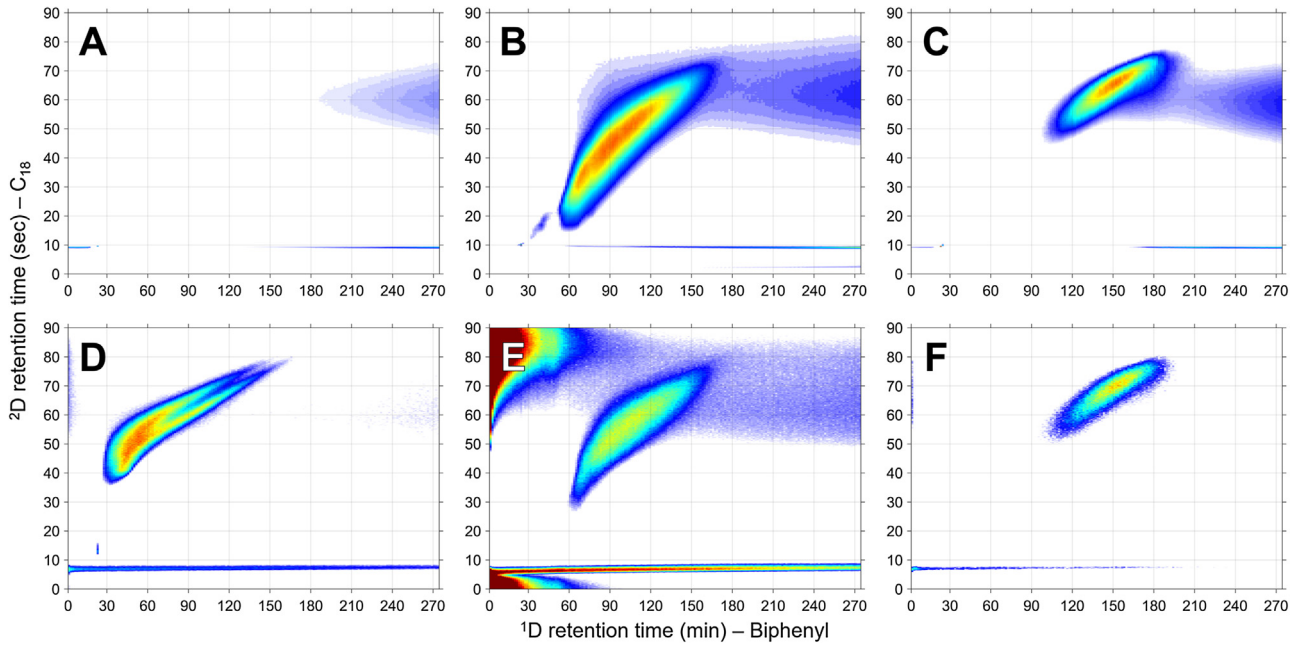

Fig. 8. LC × LC-UV chromatograms of the saturate (A), aromatic (B) and resin (C) fractions of maltenes, shown at a detection wavelength of 340 nm, and LC × LC-CAD chromatograms of the saturate (D), aromatic (E) and resin (F) fractions of maltenes. The chromatograms were recorded according to the method described in Section 2.4.6.

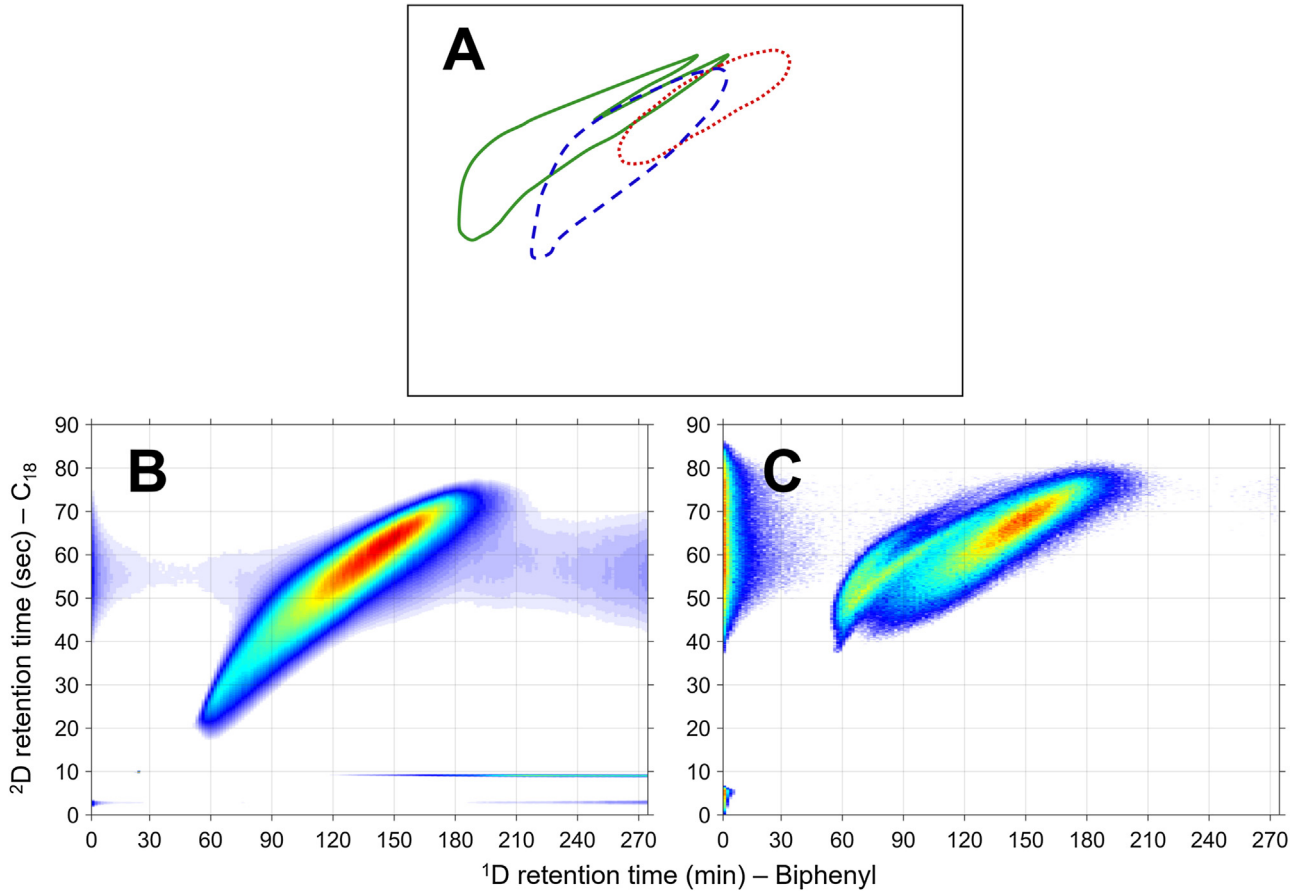

Fig. 9. (A) Overlay of the contours of the saturate (green, solid line), aromatic (blue, dashed line) and resin (red, dotted line) fractions of maltenes detected using a CAD as seen in Fig. 7. LC × LC-UV (B) chromatogram of the maltenes, shown at a detection wavelength of 340 nm and LC × LC-CAD (C) chromatogram of the maltenes. The chromatograms were recorded according to the method described in Section 2.4.6.

their retention parameters. Pinpointing the retention times of specific components in a sample which contains such a multitude of components has been attempted by fractionating the sample and re-injecting well-separated fractions into the fast and slow gradient runs, essentially creating artificial peak maxima. Since the peak maxima of fractions will be selected as input rather than the peak maxima of specific components, further investigation outside the scope of this study is required to determine whether this approach is applicable.

4. Conclusions

An initial separation of heavy oil using LC × LC has been achieved. Saturates were separated from the aromatics and resins, although, the latter were not resolved fully. The choice of stationary phases and the respective selectivity obtained for the samples remain the limiting factors for obtaining informative separations.

PIOTR was applied to a standard mixture of polycyclic aromatic hydrocarbons and to an aromatic extract of hydrowax. This showed promise, but it is not yet possible to apply PIOTR to samples that do not yield distinct peaks. To develop our understanding of the maltenes further it would be useful to apply PIOTR. The retention parameters obtained through this program can provide insight into the behavior and, consequently, the nature of components within a certain separation space. A possible way to enable the tracking of peaks between the fast and slow runs needed as input for PIOTR would be to fractionate the sample. Re-injecting fractions that were collected with sufficient time between them in both the fast and slow run will allow tracking of the fraction maxima. PIOTR could be applied on these maxima and be used to optimize the gradients. Although this may seem like a simple solution it does require quite a bit more time than just the collection of two LC × LC chromatograms, which is one of the key assets of PIOTR.

Another way to improve our understanding of the maltenes sample as well as its separation, would be to attach an MS to the end of the system. However, the nature of the sample may complicate this hyphenation. The complexity of the sample and the myriad of components present may cause matrix effects as well as preferred or suppressed ionization of specific species. Nevertheless, the addition of the MS data would make the application of PIOTR a lot easier, since it would allow for specific components to be tracked according to their mass-to-charge ratio.

Acknowledgements

The authors wish to thank Gwen Philibert, Bob Szentirmay, Bill Reppart and Ron Skelton from Shell Global Solutions International (Houston, TX, USA) as well as the Amsterdam analytical team for their interest and constructive feedback. Additionally the authors would like to thank Frans van den Berg (formerly from Shell Global Solutions International (Amsterdam, NL)) for making this research possible.

This publication has been written within the context of the MAnIAC project which is funded by the Netherlands Organization for Scientific Research (NWO) in the framework of the Programmatic Technology Area PTA-COAST3 of the Fund New Chemical Innovations [Project 053.21.113].

Appendix A. Supplementary data

Supplementary material related to this article can be found, in the online version, at doi:https://doi.org/10.1016/j.chroma.2018.06.001.

References

[1] W.R. Epperly, L.E. Swabb, J.W. Taunton, Exxon donor solvent coal liquefaction process, JPL Proc. Conf. Coal Use Calif. (1978) 268–272.
[2] B. Scheffer, M.A. Van Koten, K.W. Röbschläger, F.C. De Boks, The shell residue hydroconversion process: development and achievements, Catal. Today 43 (1998) 217–224.
[3] J. Stommel, B. Snell, Consider better practices for refining operations, Hydrocarb. Process. 86 (2007) 105–109.
[4] J.F. McKay, P.J. Amend, P.M. Harnsberger, T.E. Cogswell, D.R. Latham, Separation and analyses of petroleum residues, Am. Chem. Soc. Div. Fuel Chem. Prepr. 21 (1976) 52–58.
[5] J.F. McKay, D.R. Latham, High performance liquid chromatographic separation of olefin, saturate, and aromatic hydrocarbons in high-boiling distillates and residues of shale oil, ACS Div. Fuel Chem. Prepr. 52 (1980) 1618–1621.
[6] J.G. Speight, Handbook of Petroleum Product Analysis, John Wiley & Sons, Inc., Hoboken, New Jersey, 2002.
[7] ASTM International, ASTM D3279-12 Standard Test Method for n-Heptane Insolubles, 2012.
[8] G. Philibert, R. Szentirmay, W. Reppart, Characterization of asphaltenes fractions using two dimensional liquid chromatography, in: 247th Am. Chem. Soc. Natl. Meet., Dallas, Texas, 2014.
[9] G. Vivó-Truyols, S. Van Der Wal, P.J. Schoenmakers, Comprehensive study on the optimization of online two-dimensional liquid chromatographic systems considering losses in theoretical peak capacity in first- and second-dimensions a pareto-optimality approach, Anal. Chem. 82 (2010) 8525–8536.
[10] Y.J. Cho, J.-G. Na, N.-S. Nho, S.H. Kim, S. Kim, Application of saturates, aromatic, resins and asphaltenes crude oil fractionation for detailed chemical characterization of heavy crude oils by fourier transform ion cyclotron resonance mass spectrometry equipped with atmospheric pressure photoionization, Energy Fuel 26 (2012) 2558–2565.
[11] A.G. Marshall, T. Chen, 40 years of fourier transform ion cyclotron resonance mass spectrometry, Int. J. Mass. Spectrom. 377 (2015) 410–420.
[12] A.G. Marshall, R.P. Rodgers, Petroleomics: chemistry of the underworld, Proc. Natl. Acad. Sci. 105 (2008) 18090–18095.
[13] T. Dutriez, M. Courtiade, D. Thiébaut, H. Dulot, F. Bertoncini, J. Vial, M.C. Hennion, High-temperature two-dimensional gas chromatography of hydrocarbons up to nC60 for analysis of vacuum gas oils, J. Chromatogr. A 1216 (2009) 2905–2912.
[14] T. Dutriez, M. Courtiade, D. Thiébaut, H. Dulot, M.C. Hennion, Improved hydrocarbons analysis of heavy petroleum fractions by high temperature comprehensive two-dimensional gas chromatography, Fuel 89 (2010) 2338–2345.
[15] Y. Hirata, F. Ozaki, Comprehensive two-dimensional capillary supercritical fluid chromatography in stop-flow mode with synchronized pressure programming, Anal. Bioanal. Chem. 384 (2006) 1479–1484.
[16] H.E. Schwartz, R.G. Brownlee, M.M. Boduszynski, F. Su, Simulated distillation of High-boiling petroleum fractions by capillary supercritical fluid chromatography and vacuum thermal gravimetric analysis, Anal. Chem. 59 (1987) 1393–1401.
[17] T. Dutriez, M. Courtiade, J. Ponthus, D. Thiébaut, H. Dulot, M.C. Hennion, Complementarity of fourier transform ion cyclotron resonance mass spectrometry and high temperature comprehensive two-dimensional gas chromatography for the characterization of resin fractions from vacuum gas oils, Fuel 96 (2012) 108–119.
[18] M. Gilar, P. Olivova, A.E. Daly, J.C. Gebler, Orthogonaliy of separation in two-dimensional liquid chromatography, Anal. Chem. 77 (2005) 6426–6434.
[19] J.C. Giddings, Maximum number of components resolvable by gel filtration and other elution chromatographic methods, Anal. Chem. 39 (1967) 1027–1028.
[20] P.J. Marriott, P.J. Schoenmakers, Z.-Y. Wu, Nomenclature and conventions in comprehensive multidimensional chromatography - an update, LCGC Eur. 25 (2012) 266–275.
[21] P. Dugo, M. del Mar Ramírez Fernández, A. Cotroneo, G. Dugo, L. Mondello, Optimization of a comprehensive two-dimensional normal-phase and reversed-phase liquid chromatography system, J. Chromatogr. Sci. 44 (2006) 561–565.
[22] K. Horie, H. Kimura, T. Ikegami, A. Iwatsuka, N. Saad, O. Fiehn, N. Tanaka, Calculating optimal modulation periods to maximize the peak capacity in two-dimensional HPLC, Anal. Chem. 79 (2007) 3764–3770.
[23] J.C. Giddings, Concepts and comparisons in multidimensional separation, J. High. Resolut. Chromatogr. Chromatogr. Commun. 10 (1987) 319–323.
[24] M. Gilar, A.E. Daly, M. Kele, U.D. Neue, J.C. Gebler, Implications of column peak capacity on the separation of complex peptide mixtures in single- and two-dimensional high-performance liquid chromatography, J. Chromatogr. A 1061 (2004) 183–192.
[25] R.M.B.O. Duarte, A.C. Barros, A.C. Duarte, Resolving the chemical heterogeneity of natural organic matter: new insights from comprehensive two-dimensional liquid chromatography, J. Chromatogr. A 1249 (2012) 138–146.
[26] T. Murahashi, Comprehensive two-dimensional high-performance liquid chromatography for the separation of polycyclic aromatic hydrocarbons, Analyst 128 (2003) 611.

[27] S.S. Jakobsen, J.H. Christensen, S. Verdier, C.R. Mallet, N.J. Nielsen, Increasing flexibility in two-dimensional liquid chromatography by pulsed elution of the first dimension: a proof of concept, Anal. Chem. 89 (2017) 8723–8730.
[28] P. Česla, T. Hájek, P. Jandera, Optimization of two-dimensional gradient liquid chromatography separations, J. Chromatogr. A 1216 (2009) 3443–3457.
[29] P.J. Schoenmakers, G. Vivó-Truyols, W.M.C. Decrop, A protocol for designing comprehensive two-dimensional liquid chromatography separation systems, J. Chromatogr. A 1120 (2006) 282–290.
[30] H. Gu, Y. Huang, P.W. Carr, Peak capacity optimization in comprehensive two dimensional liquid chromatography: a practical approach, J. Chromatogr. A 1218 (2011) 64–73.
[31] B.W.J. Pirok, A.F.G. Gargano, P.J. Schoenmakers, Optimizing separations in online comprehensive two-dimensional liquid chromatography, J. Sep. Sci. 41 (2018) 68–98.
[32] B.W.J. Pirok, S. Pous-Torres, C. Ortiz-Bolsico, G. Vivó-Truyols, P.J. Schoenmakers, Program for the interpretive optimization of two-dimensional resolution, J. Chromatogr. A 1450 (2016) 29–37.
[33] G. Vanhoenacker, M. Steenbeke, F. David, P. Sandra, K. Sandra, U. Huber, Analysis of Polycyclic Aromatic Hydrocarbons in Petroleum Vacuum Residues by Multiple Heart-Cutting LC Using the Agilent 1290 Infinity 2D-LC Solution, 2016.
[34] G. Vanhoenacker, F. David, P. Sandra, Profiling of Polycyclic Aromatic Hydrocarbons in Crude Oil with the Agilent 1290 Infinity 2D-LC Solution, 2015.
[35] J.C. Fetzer, W.R. Biggs, K. Jinno, HPLC analysis of the large polycyclic aromatic hydrocarbons in a diesel particulate, Chromatographia 21 (1986) 439–442.
[36] B.W.J. Pirok, S.R.A. Molenaar, R.E. van Outersterp, P.J. Schoenmakers, Applicability of retention modelling in hydrophilic-interaction liquid chromatography for algorithmic optimization programs with gradient-scanning techniques, J. Chromatogr. A 1530 (2017) 104–111.
[37] J. Beens, Chromatographic Couplings for Unraveling Oil Fractions, University of Amsterdam, 1998.
[38] L.C. Sander, M. Pursch, S.A. Wise, Shape selectivity for constrained solutes in reversed-phase liquid chromatography, Anal. Chem. 71 (1999) 4821–4830.
[39] S.A. Wise, B.A. Benner, H.C. Liu, G.D. Byrd, A. Colmsjö, Separation and identification of polycyclic aromatic hydrocarbon isomers of molecular weight 302 in complex mixtures, Anal. Chem. 60 (1988) 630–637.